

Article

CoMP-Aware BBU Placements for 5G Radio Access Networks over Optical Aggregation Networks

Ahmed M. Awad ^{1,*} , Mohamed Shehata ¹, Safa M. Gasser ¹ and Hesham EL-Badawy ² 

¹ Department of Electronics and Communication Engineering, Arab Academy for Science, Technology and Maritime Transport (AASTMT), Cairo 11799, Egypt

² Network Planning Department, National Telecommunication Institute (NTI), Cairo 11432, Egypt

* Correspondence: ahmedawad@student.aast.edu

Abstract: The huge traffic demand envisioned in 5G requires radical changes in mobile network architecture. A Centralized Radio Access Network (C-RAN) was introduced as a novel mobile network architecture, designed to effectively support the challenging requirements of future 5G networks. Coordinated Multi-point (CoMP) is one of the technologies aiming to increase user traffic by transforming inter-cell interference into useful signals to maximize cell-edge users throughput. Intra-CoMP means that cooperating RRHs are assigned to the same Base Band Unit (BBU). On the other hand, in inter-CoMP, the cooperating RRHs are assigned to different BBUs, which introduce overhead signalling over an X2 interface. This paper proposes a model for BBU placement in C-RAN deployment over a 5G optical aggregation network. The model aims to minimize the number of users undergoing inter-CoMP, therefore reducing X2 signalling overhead. First, we solve the BBU placement problem using Integer Linear Programming (ILP), which minimizes the number of BBUs and the number of used links. Second, given the output of the ILP model (i.e., BBU locations and routes), we propose a heuristic algorithm to reconfigure the BBUs (i.e., the assignment of the RRHs to their corresponding BBUs), which aims at minimizing the number of users undergoing inter-CoMP. The proposed heuristic algorithm considers minimizing end-to-end delay, the number of used wavelengths, and maximizing multiplexing gain. The results show that up to 97% of inter-CoMP users migrated to intra-CoMP users. This results in a decrease in the X2 traffic, which is mainly used for the coordination between the BBUs.

Keywords: Cloud-RAN; CoMP; 5G network; edge users; optical aggregation; fronthaul; X2 interface



Citation: Awad, A.M.; Shehata, M.; Gasser, S.M.; EL-Badawy, H. CoMP-Aware BBU Placements for 5G Radio Access Networks over Optical Aggregation Networks. *Appl. Sci.* **2022**, *12*, 8586. <https://doi.org/10.3390/app12178586>

Academic Editor: Christos Bouras

Received: 22 July 2022

Accepted: 23 August 2022

Published: 27 August 2022

Publisher's Note: MDPI stays neutral with regard to jurisdictional claims in published maps and institutional affiliations.



Copyright: © 2022 by the authors. Licensee MDPI, Basel, Switzerland. This article is an open access article distributed under the terms and conditions of the Creative Commons Attribution (CC BY) license (<https://creativecommons.org/licenses/by/4.0/>).

1. Introduction

A significant amount of research for determining specifications and architectures of a next-generation 5G mobile network has already been prompted by the exponential growth of wireless traffic. Fifth-generation mobile networks (5G) are expected to provide higher bandwidths, higher data rates with high level of security, and lower latency [1,2]. Fifth-generation networks provide various types of communication methods, such as machine-to-machine (M2M), human-to-machine (H2M), device to-device (D2D), and Internet of Things (IoT) [3,4]. In addition, recent research includes device-to-device (DoD) communication in 5G networks to maximize throughputs [5]. One proposed network architecture that promises to meet the 5G requirements is the Centralized Radio Access Network (C-RAN). Unlike Distributed RAN (D-RAN) architecture, where the processing units are placed together with the RF antennas in cell sites, in C-RAN, multiple baseband processing units (BBUs) are placed in a central location called BBU pool [6].

Several Remote Radio Heads (RRH) are linked to the BBU pool via an optical transmission network that supports the 'front-haul' deployed according to a given radio planning strategy [6,7]. The BBU pool is connected to the core network through 'back-haul' links.

C-RAN promises to allow for a substantial multiplexing gain in terms of hardware and processing power of the BBUs. Several studies have been conducted to examine the

cost savings achieved by C-RANs from the point of view of Capital Expenditure (CapEx), Operating Expenditure (OpEx), and Total Cost of Ownership (TCO). Compared to D-RAN, C-RAN reduce the TCO up to 68% [8].

Despite the advantages offered by C-RAN, the front-haul network must have a very high bandwidth and very low latency, resulting in high transport-network costs. Optical aggregation networks based on wavelength division multiplexing (WDM) are considered to be the suitable candidate solution for meeting the requirements of the front-haul [9,10].

C-RAN represents a convenient environment for applying advanced radio coordination techniques such as Coordinated Multi-Point (CoMP) Transmission/Reception, as D-RAN does not satisfy the tight latency constraint of the CoMP techniques (1 msec) [11]. CoMP is suggested as a promising mobile communication technology released in LTE-Advanced Rel-11 to enhance cell-edge user throughput by transforming inter-cell interference into useful signals. It falls into two main categories: Joint Processing (JP) and Coordinated Scheduling or Beamforming (CS/CB). Firstly, JP occurs when coordination exists between multiple base stations that transmit/receive simultaneously to/from the UEs using the same frequency and time resources at the cell edge. Second, CS/CB is a form of coordination where the adjacent cell sites cooperate by allocating different frequencies and beams at the cell edge [12].

From the point of view of the BBU pools, CoMP services can be classified into two types: (i) inter-BBU CoMP and (ii) intra-BBU CoMP. First, in inter-BBU CoMP, each cooperative RRH is linked to a different BBU, which means that the signaling data will be exchanged between the different BBUs over an X2 interface. This imposes a large back-haul bandwidth requirement. Second, in intra-BBU CoMP, Cooperative RRHs are connected to a single BBU. This eliminates signaling data exchanges, which result in saving bandwidth and reducing latency.

In this paper, we discuss the BBU placement problem for C-RAN deployment over 5G optical aggregation networks, taking into consideration a reduction in the number of RRHs undergoing inter-CoMP. The main contribution of this paper is the decrease in the number of inter-CoMP users, which will save the X2 interface signalling overhead as well as provide improved coordination between RRHs engaged in CoMP. Moreover, we aim to reduce the number of BBU pools and the number of wavelengths used. This is performed by implementing two steps:

First, we formulate an ILP optimization problem for BBU placement for C-RAN over a 5G optical aggregation network. We consider a multi-objective optimization problem, which minimizes (i) the number of BBU pools and (ii) the number of wavelengths used. The ILP results in the optimum location of the BBU pools' traffic routing. In addition, it pairs each RRH with a corresponding BBU pool.

Second, after knowing the ILP outputs (i.e., BBU pool locations, traffic routing and RRHs/BBU pools pairing), we propose a heuristic algorithm to reduce the number of users undergoing inter-CoMP services. This is performed as follows: For the RRHs engaged in inter-CoMP service, we reconfigure their serving BBU pools and reroute them to different BBU pools such that the new serving BBU pool enables the RRH to be engaged in intra-CoMP services. The heuristic algorithm changes the serving BBU of the RRH dynamically to decrease the number of inter-CoMPs. The new serving BBU pool is chosen based on three criteria: (i) BBU computational capacity; (ii) the number of newly activated links; (iii) path delay. Decreasing the number of inter-CoMP users will save the X2 interface signalling overhead as well as provide better coordination between RRHs engaged in CoMP. The algorithm performance is a measure in terms of the number of users transferred from inter-CoMP to intra-CoMP, as well as the number of activated BBU pools and the number of used wavelengths. The results show that at low latency (50 μ sec), up to 97% of inter-CoMP users migrated to be intra-CoMP users. On the other hand, at higher latencies (80 μ sec), up to 78% of inter-CoMP users migrated to be intra-CoMP users. On the other hand, optical link utilization increases up to 94% compared to the optimum solution.

The research is divided into six sections. Related studies are discussed in Section 2. The proposed ILP BBU placement problem is discussed in Section 3. The proposed heuristic placement algorithm for CoMP is tackled in Section 4. The results are shown in Section 5. A conclusion of the work is provided in Section 6.

2. Related Work

C-RAN has been studied intensely in the literature. The concept of C-RAN has attracted the attention of many researchers. For example, the authors of [13] provided a comprehensive survey on the recent research direction of C-RAN. In [14], the authors propose a model to optimize the energy consumption of Heterogenous C-RAN (H-CRAN). The model considers the energy consumption of radio access points (RAPs), fronthaul, and the BBU pool. In [15], the authors propose a novel resource allocation model that optimizes the energy consumption of a C-RAN. The resource allocation problem is split into two subproblems—namely, the Bandwidth Power Allocation (BPA) and the BBU Energy-Aware Resource Allocation (EARA). In [8], the authors propose an analytical model to evaluate the multiplexing gain obtained from deploying C-RAN compared to the Distributed RAN (D-RAN).

In C-RAN, the front-haul network restricted requirements in terms of end-to-end delay and data rate [16], which led to the introduction of optical aggregation networks based on wavelength division multiplexing (WDM) as an efficient solution to fulfill the aforementioned requirements. In this context, several studies have discussed the BBU placement problem using both ILP model. In [17], the authors introduce a BBU placement optimization problem over WDM aggregation networks using ILP to minimize the deployment cost. The model is not limited for BBU placement but also the electronic switches placement. The authors compare between the impact of two different fronthaul transport options, Optical Transport Network (OTN) and Overlay, on BBU centralization. The authors in [18] propose a cost-efficient placement model for RRHs, BBUs and optical fiber in 5G Radio-Optical communication Networks (5G-RONs). The problem is formulated using ILP. The authors aim to solve the problem taking into consideration achieving certain level of population coverage. The authors discuss the difficulty of practical solving ILP models in 5G-RONs scenarios. Similarly, authors in [19] propose a model for BBU placement that optimizes the total cost of ownership (TCO) using ILP under different delay thresholds. They considered the Time and Wavelength Division Multiplexing Passive Optical Network (TWDM-PON) as a fronthaul with different splitting ratios. In [20], the authors propose TWDM-PON architecture to support both the fronthaul network of the Cloud-Fog Radio Access Network (CF-RAN) and the interconnection of cell-sites to the fog nodes. The authors propose an ILP model that decides the number of fog nodes necessary for accommodating all traffic demands and where to process them considering TWDM-PON's capacity and the best overall network energy performance.

The BBU placement problem is investigated using different heuristic algorithms to solve the problem for large network scenarios. In [21], the authors propose a BBU placement model considering different functional split options. The authors aimed to reduce the fronthaul latency and minimized cost reductions. They formulated an ILP optimization problem and then developed a heuristic algorithm proposed to solve the proposed model for large network scenarios. In [22], the authors present a model to optimize the storage allocation problem and content placement problem jointly in a hierarchical cache-enabled C-RAN architecture for IoT sensing services. They formulate the joint problem as an integer linear programming (ILP) model with the objective to minimize the total network's traffic cost. Then, two heuristic algorithms were proposed in order to reduce the computational complexity of ILP. In [23], the authors tackle the BBU placement problem while considering network survivability. The authors propose an ILP optimization problem to determine the primary and secondary locations of the BBU pools, as well as the primary and secondary paths between the RRH and BBU pool. Similar studies were conducted in [24] while using heuristic algorithms. The authors in [25] proposed an efficient dynamic-resource

infrastructure management algorithm based on a combination of Markov-Process and Time Division Multiple Access (TDMA) protocols in Software-Based Networks. In [26], the authors co-located the BBU pool with an edge cloud at the so-called BBU node. They proposed a heuristic algorithm to allocate the users' tasks to the BBU nodes and to route the traffic from the RRH to that node. Then, they solved the problem by taking into consideration survivability concerns. They use both primary and backup BBU nodes to issue the request such that the primary path and backup path are disjointly linked.

Recently, machine learning has gained increasing attention in optimizing 5G networks. The authors in [27] used Deep Reinforcement Learning (DRL) algorithms to solve Base Band Function (BBF) placements and routing in C-RAN and Next Generation RAN (NG-RAN). The authors show that DRL enables the network operator to solve the problem dynamically according to the traffic demand. In [28], the authors developed a model to allocate the RRH to a certain BBU pool in the C-RAN. The model is based on a deep neural network algorithm that can accurately predict future reconfigurable optical add-drop multiplexer (ROADM) network resource requirements.

Several studies have been conducted in the literature investigating the CoMP performance in different mobile technologies (e.g., 4G and 5G). CoMP in 4G LTE networks has been widely investigated; in [29], the authors show that CoMP leads to network throughput and capacity expansions in LTE-A. They show the enhancement in terms of spectral efficiency through cooperative coordination strategies. In [30], the authors propose a CoMP model that demonstrates the performance of an LTE-A network at the cell edge for high capacities in order to improve the throughput and spectral efficiency. In [31], the authors designed an adaptive online learning approach and smart access for CoMP with carrier aggregation in order to improve network performance. In [32], the authors propose different scenarios of the CoMP model dealing with backhaul traffic in order to improve network throughputs in LTE-A network. In [33], the authors propose an algorithm to coordinate the clusters of the cells as well as a Radio Coordination Controller (RCC) placement optimization problem. This results in an overall improvement in CoMP performance.

More studies related to our research on CoMP in 5G networks are intensely discussed. In [34], the study discusses the enhancement of user throughput in C-RAN by distributing the available resources of cooperative cells among CoMP and non-CoMP users. In [35], the authors propose a novel JT-CoMP scheme with a path loss model to minimize the network's back-haul traffic. The authors in [36,37] integrate CoMP with NOMA in order to improve the cell edge users' performance. In [38], the authors study CoMP joint transmission clustering problems by taking into consideration the caches at base stations and mmWave mesh backhaul. The authors propose a heuristic algorithm to minimize the back-haul traffic while achieving the data rate requirement of each user. In [39], the authors study the effect of CoMP transmission on Ultra-dense networks (UDNs) complexity and transmission delay with collaboration among Mobile Edge Computing (MEC) servers. In [40], the authors propose a C-RAN system model with dynamic clustering approaches in order to reduce the inter-cluster interference. In [41], the authors investigate a joint beamforming coordination and user-selection problem on CoMP-based New Radio-Unlicensed (NR-U) networks. The authors propose an optimum solution and suboptimum solution in order to solve Mixed-Integer Non-Linear Programming (MINLP) problems. In [42], the authors propose deep learning algorithms in order to improve the performance of Downlink-coordinated Multipoint (DL-CoMP) in heterogeneous 5G New Radio (NR) networks. In [43], the authors propose User-Centric Clustering algorithms in order to select UEs that will operate JT-CoMP. the results show the enhancement overall system throughput as well as edge users throughput. In [44], the authors propose an ILP to coordinate the clusters of the cells as well as a Radio Coordination Controller (RCC) placement optimization problem in order to maximize the overall network's throughput. In [45], the authors discussed the cell edge users' throughput considering CoMP while minimizing the data exchange (X2 interface) between BBU pools by configuring the front-haul network. The authors proposed two heuristic algorithm graph-based lightpath reconfigurations (MCG-LR) and a

BBU weight-based lightpath reconfiguration (BW-LR). The results show the improvement of the elastic radio resources. However, the authors did not take into consideration the BBU placement problem and delay requirements.

Finally, to the best of our knowledge, this is the first study to solve the BBU placement problem by taking into consideration the minimization of the number of inter-CoMP users.

3. Problem Formulation

The problem of BBU pool placement is described as follows [23]:

Given: Network topology, number of wavelengths per connection, maximum allowable front-haul latency, and computational effort required by a pool serving given the number of cell sites;

Output: Placement of BBUs so that BBU pools are connected to several RRHs;

Objective: Minimizing the following:

- i. The number of BBU pools;
- ii. The number of fiber connections used.

3.1. Input Sets and Parameters

The input sets and parameters of the BBU placement problem are described as follows in Table 1;

Table 1. Input sets and parameters.

| Inputs | Description |
|----------|---|
| N | Set of nodes in the physical network, $i, j, m, n \in N$ |
| S_p | Set of physical links, $i - j \in S_p$ |
| S_v | Set of virtual links, $m - n \in S_v$ |
| d_{ij} | The propagation delay introduced by the physical link $i - j$ |
| D | The maximum allowable delay between cell site and the BBU pool |
| W | The number of wavelengths per each physical link |
| C_q | The computational effort in GOPS needed by a pool if it serves q RRHs |
| C | The maximum computational effort in GOPS that can be accommodated by a pool |

3.2. Decision Variables

The decision variables of the BBU placement problem are described as follows in Table 2;

Table 2. Decision Variables.

| Variable | Description |
|-------------------|--|
| $K_i = 1$ | If node i hosts a BBU pool (binary) |
| $X_{i,m} = 1$ | If cell site m is assigned to a BBU pool at node i (binary) |
| $Y_{ij}^{mn} = 1$ | If virtual link $m - n \in S_v$ between cell site placed at node m and BBU pool placed at node n is routed over physical link $i - j \in S_p$ (binary) |
| $b_{i,q} = 1$ | If the BBU pool hosted by node i serves q RRHs (binary). If node i does not host a pool, then $b_{i,0} = 1$ (binary). |

Figure 1 shows the difference between the physical link and the virtual link. In this example, the virtual link, A-G, is routed over physical links A-B, B-C, and C-G. Therefore, Y_{AB}^{AG} , Y_{BC}^{AG} , and Y_{CG}^{AG} equal one, while Y_{ij}^{AG} for $ij \neq AB, BC, CG$ equal zero.

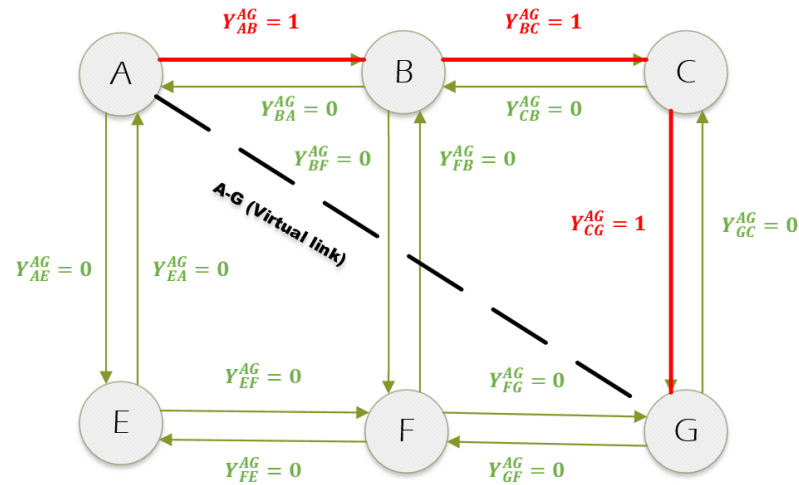


Figure 1. Routing the virtual link over physical links.

3.3. Objective Function

The multi-objective function is formulated in Equation (1), consisting of two terms. The first term minimizes the number of BBU pools, while the second minimizes the number of used wavelengths in the transport network:

$$\min \left(\beta \sum_i K_i + \gamma \sum_{ij} \sum_{mn} Y_{ij}^{mn} \right) \tag{1}$$

where, β and $\gamma \in [0.1]$ can be tuned to select the primary and secondary objectives of the optimization function.

3.4. Constraints

The constraints are discussed as follows;

$$\sum_i X_{i,m} = 1 \quad \forall m \tag{2}$$

$$\sum_q b_{i,q} = 1 \quad \forall i \tag{3}$$

$$\sum_q qb_{i,q} = \sum_m X_{i,m} \quad \forall i \tag{4}$$

$$\sum_j (Y_{ij}^{mn} - Y_{ji}^{mn}) = \begin{cases} X_{n,i}, & \text{if } i = m, m \neq n. \\ -X_{i,m}, & \text{if } i = n, m \neq n. \\ 0, & \text{otherwise.} \end{cases} \quad \forall mn, \forall i \tag{5}$$

Equation (2) ensures that exactly one BBU pool is associated with every RRH. Equation (3) and Equation (4) ensure that the number of RRHs served by Pool i equals the sum of RRHs assigned to that pool i . Equation (5) ensures that physical links are mapped to all virtual links connecting the RRHs to the BBU pool.

$$X_{i,m} \leq 1 \quad \forall i, \forall m \tag{6}$$

$$K_i \geq \frac{\sum_m X_{i,m}}{M}, \quad \forall m \tag{7}$$

$$\sum_q b_{i,q} C_q \leq C \quad \forall i \tag{8}$$

$$\sum_{mn} Y_{ij}^{mn} \leq W \quad \forall ij \quad (9)$$

$$\sum_{ij} Y_{ij}^{mn} d_{ij} \leq D \quad \forall mn \quad (10)$$

Equation (6) ensures that the BBU pool for the same RRH is at different nodes. Equation (7) identifies the node as a BBU pool if it hosts one RRH. Equation (8) ensures that computation processing required by the base station hosted in a BBU pool does not exceed the computational capacity of this BBU pool. Equations (9) and (10) guarantee the link capacity and the delay requirements are met, respectively.

The model in [46] is used to determine the computational effort needed by each cell site. This is expressed in Giga Operations Per Second (GOPS). First, we choose a statistical distribution (namely normal or uniform) to model the spatial distribution of mobile users in a given serving area. Then, we allocate the users to their serving cell sites according to a realistic user-cell site-association strategy. After that, we apply a scheduling algorithm to distribute physical resource blocks of the eNB among its attached users. Then, we calculate the computational effort per user after knowing his channel condition, used resources, modulation, code rate, and MIMO mode.

4. CoMP Aware BBU Placement Algorithm

As stated earlier, the contribution of this paper is divided into two parts. First, we optimize the placement of the BBU pool. Second, we reconfigure the CoMP inter BBU into CoMP intra-BBU. Thus, we construct a heuristic algorithm for the reconfiguration phase. This is illustrated in Figure 2. The heuristic algorithm has following steps:

1. Based on the optimization problem explained in Section 3, we use outputted BBUs locations and the routing as the initial solution.
2. We distribute the users uniformly on the given area.
3. We classify the users to CoMP users and non-CoMP users based on their location with respect to the cell's center. Given that the cell's radius equals 500 m if the distance between the user and the cell center is less than 80 % from cell radius, the user is considered as a non-CoMP user. Otherwise, the user is considered as a CoMP user (i.e., the user is near the cell edge).
4. We find the cell edge with the highest number of CoMP users; then, we change the serving BBU according to the algorithm explained below.

Assume two coordinated RRHs: *RRH a* and *RRH b*. If *RRH a* is served by the *BBU pool a* while *RRH b* is served by the *BBU pool b*. The objective is to re-allocate the two RRHs so that they are served by the same BBU to undergo intra-CoMP instead of inter-CoMP. Choosing the RRH that will change its serving BBU will be performed based on the following aspects: (i) maximizing the multiplexing gain (Case 1 and Case 2), (ii) minimizing the number of active fiber links (Case 3 and Case 4), and (iii) minimizing the end-to-end delay between the RRHs and the BBUs (Case 5 and Case 6). This is considered in the following six cases. In the following, we will use the terminology *path 1* as the path between *RRH a* and *BBU pool b*. On the other hand, *path 2* is the path between *RRH b* and *BBU pool a*.

- **Case 1:**
- As shown in Algorithm 1, if the delay of *path 1* is less than the maximum allowable delay **AND** if the delay of *path 2* is less than the maximum allowable delay, then the following is the case:
 - Condition 1: Condition of BBU Computational Capacity: choose the serving BBU (i.e., *BBU pool a* or *BBU pool b*) for the two coordinated RRHs (i.e., *RRH a* or *RRH b*) based on the BBU that accommodates more RRHs and then end the process. If two BBUs accommodate the same number of RRHs, then the following is the case:
 - Condition 2: Condition of the number of active links: choose the serving BBU (i.e., *BBU pool a* or *BBU pool b*) for the two coordinated RRHs (i.e., *RRH a* or *RRH b*)

b) based on the path (i.e., *path 1* or *path 2*) with the minimum number of new activated fiber links and then end the process. If the two paths have the same path delay, then the following is the case:

- Condition 3: Condition of the link Delay: choose the serving BBU (i.e., *BBU pool a* or *BBU pool b*) for the two coordinated RRHs (i.e., *RRH a* or *RRH b*) based on the path (i.e., *path 1* or *path 2*) with minimum path delay then end. If the two paths have the same path delay, then the reconfiguration is unavailable and the RRHs will undergo inter-CoMP.
- If the delay of *path 1* ONLY less than the maximum allowable delay, then choose *BBU pool b* as the serving BBU for the two coordinated RRHs (BBU pool in *path 1*). Then end
- If the delay of *path 2* ONLY less than the maximum allowable delay, then choose *BBU pool a* as the serving BBU for the two coordinated RRHs (BBU pool in *path 2*). Then, end the process.
- Otherwise, the reconfiguration is unavailable and the RRHs will undergo inter-CoMP.

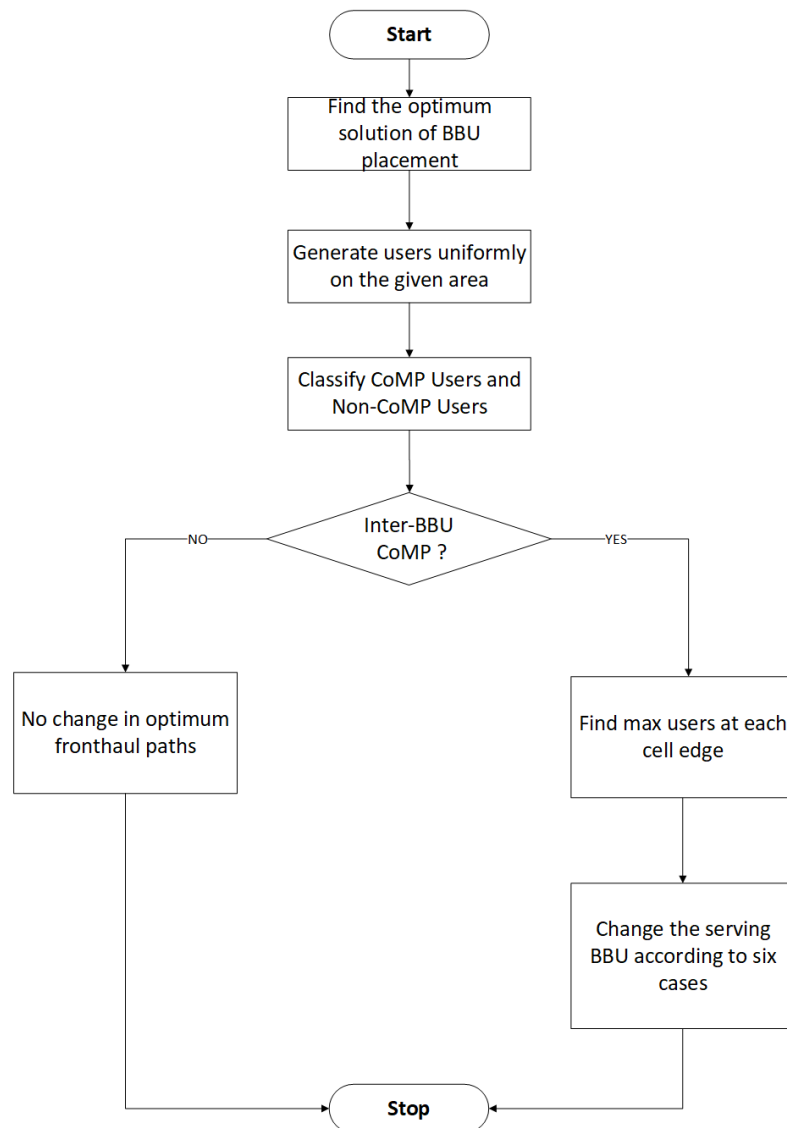


Figure 2. CoMP-aware BBU placement algorithm.

The pseudo-code for case 1 is shown below.

Algorithm 1: Pseudo Code for case 1**Input:** Optimum results of BBU Placement**Output:** Reconfigurable placement RRH-BBU

```

1: Initialization
   i.  $U_{Inter}$  : Number of inter-BBU CoMP users between two given RRHs.
   ii.  $Path1$  : Shortest path from RRH a to BBU pool b.
   iii.  $Path2$  : Shortest path from RRH b to BBU pool a.
   iv.  $BBU_{CapA}$  : Number of RRHs accommodated by BBU a.
   v.  $BBU_{CapB}$  : Number of RRHs accommodated by BBU b.
   vi.  $L_1$  : Number of the new activated fiber links needed if we use  $path1$ .
   vii.  $L_2$  : Number of the new activated fiber links needed if we use  $path2$ .
   viii.  $D$  : Max allowable latency.
   ix.  $D_1$  : Total latency experienced in path 1.
   xi.  $D_2$  : Total latency experienced in path 2.
2: For each RRH: find max  $U_{Inter}$  in each edge of cell, do
3:   Find  $BBUa$  and  $BBUb$ 
4:   If  $D_1 < D$  and  $D_2 < D$ , do
5:     If  $BBU_{CapA} > BBU_{CapB}$ , do
6:        $Finalselection_{1st\ case} = BBU\ pool\ a$ 
7:     Else if  $BBU_{CapA} < BBU_{CapB}$ , do
8:        $Finalselection_{1st\ case} = BBU\ pool\ b$ 
9:     Else if  $L_1 < L_2$ , do
10:       $Finalselection_{1st\ case} = BBU\ pool\ b$ 
11:    Else if  $L_1 > L_2$ , do
12:       $Finalselection_{1st\ case} = BBU\ pool\ a$ 
13:    Else if  $D_1 < D_2$ , do
14:       $Finalselection_{1st\ case} = BBU\ pool\ b$ 
15:    Else
16:       $Finalselection_{1st\ case} = BBU\ pool\ a$ 
17:    End if
18:   Else if  $D_1 < D$ , do
19:      $Finalselection_{1st\ case} = BBU\ pool\ b$ 
20:   Else if  $D_2 < D$ , do
21:      $Finalselection_{1st\ case} = BBU\ pool\ a$ 
22:   Else
23:     No path available
24:   End if
25: End For

```

All other cases are as explained in case 1 except for the order of conditions. All different cases are summarized in Table 3.

Computational Complexity

We evaluate the problem complexity for ILP optimization problem, it explained as the following steps. First, we evaluate the total number of variables for objective function, it is expressed as the following:

$$N_v = |N|(1 + S_v S_p) \quad (11)$$

We can neglect the constant, so it becomes as following:

$$N_v = |N|(|S_v| \cdot |S_p|) \quad (12)$$

Second, we evaluate the number of constraints, it expressed as the following:

$$N_{vconst} = |N|(6 + S_v) + S_p + S_v \quad (13)$$

We can neglect the constant and summarize with the dominate part, so it becomes as following:

$$N_{vconst} = |N| \cdot |S_v| \quad (14)$$

Therefore, the complexity order are the summation the number of variables and number of constraints.

$$O(|N| \cdot |S_p| \cdot |S_v|) \quad (15)$$

The problem complexity for heuristic algorithm is expressed as

$$O(|N|) \quad (16)$$

Table 3. Different cases for the heuristic algorithm

| | Condition 1 | Condition 2 | Condition 3 |
|---------------|---|---|---|
| Case 1 | Condition of BBU computational capacity | Condition of the number of active links | Condition of the link Delay |
| Case 2 | Condition of BBU computational capacity | Condition of the link Delay | Condition of the number of active links |
| Case 3 | Condition of the number of active links | Condition of the link Delay | Condition of BBU computational capacity |
| Case 4 | Condition of the number of active links | Condition of BBU computational capacity | Condition of the link Delay |
| Case 5 | Condition of the link Delay | Condition of BBU computational capacity | Condition of the number of active links |
| Case 6 | Condition of the link Delay | Condition of the number of active links | Condition of BBU computational capacity |

5. Case Study and Results

5.1. Simulation Settings

In this section, we consider an optical aggregation network with 16 nodes uniformly distributed over a dense sub-urban region of 5 km², as shown in Figure 3. We used the same network topology as in [47]. We assume 500 users that are randomly distributed. The nodes considered are fiber-linked. We assume that each node represents a cell site and a possible BBU pool location. We take into account the fiber propagation delay and the node processing delay. The propagation delay per link (d) is considered to be 23.6 μ sec, while the node processing delay equals 20 μ sec. We assume that M is 1000. We consider two cases for the maximum number of wavelengths per physical links $W = 4$ and $W = 6$ [23]. Each RRH-BBU connection is transported over a dedicated wavelength of the so-called 'front-haul' connection. The model in [8,46] is used to determine the the computational effort needed by each cell site. This is expressed in Giga Operations Per Second (GOPS).

We optimize the number of BBU pools as a primary objective and then the number of physical links is used as a secondary objective, where α is 1, and β is 10^{-3} . We used the MATLAB optimization Toolbox on a workstation equipped with 8×2 GHz processors and 32 GB RAM. The results obtained are the average of 100 different runs.

5.2. Results

Figure 4 shows the percentage of users migrated from Inter-BBU CoMP to Intra-BBU CoMP. As the maximum allowable latency increases, the percentage of users migrating from Inter-BBU CoMP to Intra-BBU CoMP decreases. This can be explained as follows: Increasing D leads to a decrease in the number of pools, decreasing the possibility for two RRHs to be served by two different BBUs. Thus, the number of Inter BBU CoMP is relatively low at high D . It is shown that at the same D , the percentages of the migrated

users from inter-CoMP to intra-CoMP for the different six cases are nearly equal. This is due to the fact that each case checks the same criteria.

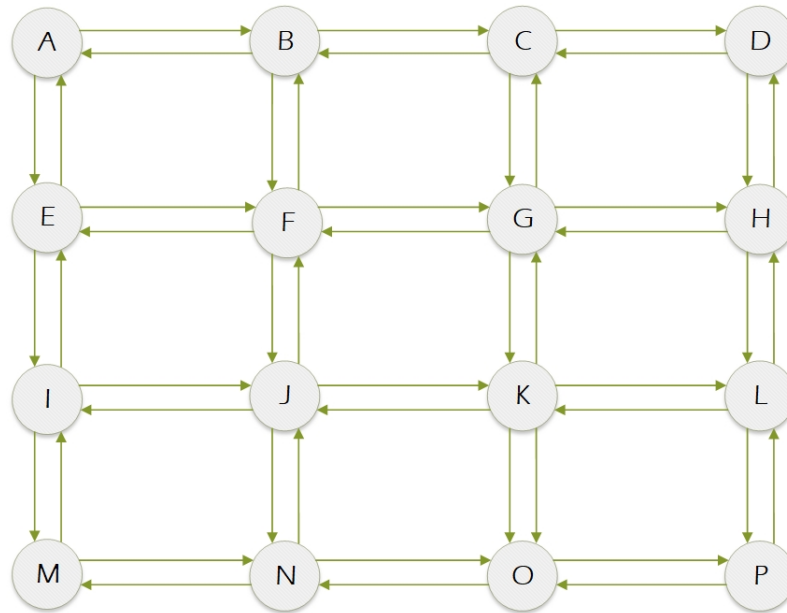


Figure 3. Network topology.

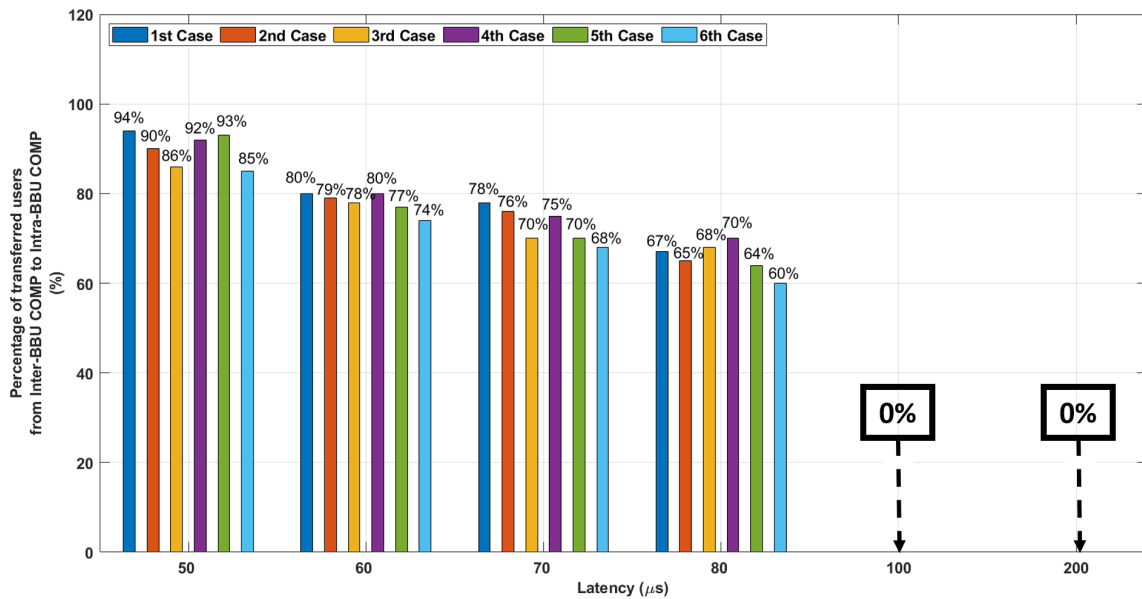


Figure 4. Percentage of transferred users from Inter-BBU CoMP to Intra-BBU CoMP (for each Cases, $W = 4$).

Figure 5 shows the number of BBU pools and the number of physical links versus different maximum allowable latency values (D_{max}) at $W = 4$. At 25 μsec and 35 μsec , there is no change in the number of BBUs and the number of physical links after the reconfigurable placement algorithm. As all BBUs are located at the cell sites, the maximum delay is not sufficient to reconfigure the RRH to be served by any other BBU. At delays equal to 50 μsec , 60 μsec , and 70 μsec , the number of BBUs does not change after reconfiguration, while the number of physical links increased by 41%, 35%, and 29% of the optimal solution, respectively. As the maximum allowable delay increases, the probability that the adjacent sites are served by the same BBU increases, leading to a higher number of intra-CoMP. Therefore, the number of migrated users decreases, and the number of sites that need

to change their served BBU decreases. At delays equaling 80 μsec , the number of BBUs decreased to two BBUs instead of three in the previous delays. This increases the number of intra-CoMP as the probability of sites being served by different BBUs decreased. Therefore, the physical links increased by 24%. At delays of 100 μsec and 200 μsec , all sites in the area are served by one BBU; thus, there is no inter-CoMP. Therefore, there is no reconfiguration and the number of physical links remains constant.

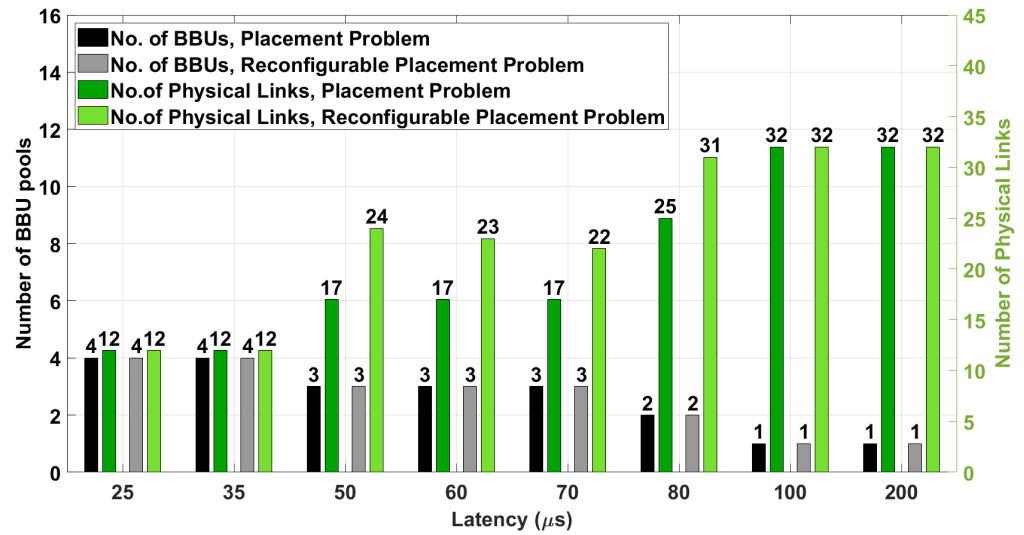


Figure 5. Number of BBU pools and physical links ($W = 4$, 1st case).

Table 4 shows the number of BBU pools and the number of physical links versus different maximum allowable latencies (D_{max}) = 50, 60, 70, and 80 μsec at $W = 4$ and $W = 6$ considering cases 2, 3, 4, 5, and 6.

Table 4. Results of other cases at 50 μsec , 60 μsec , 70 μsec , and 80 μsec .

| Cases | 50 μsec | | 60 μsec | | 70 μsec | | 80 μsec | | | | | | | | | | |
|---------|--------------------|-----------|--------------------|-----------|--------------------|-----------|--------------------|-----------|----|---|----|---|----|---|----|---|----|
| | Before | After | Before | After | Before | After | Before | After | | | | | | | | | |
| | BBU | Ph. Links | | | | | | | | | |
| $W = 4$ | 2nd | 3 | 17 | 3 | 25 | 3 | 17 | 3 | 24 | 3 | 17 | 3 | 23 | 2 | 25 | 2 | 30 |
| | 3rd | 3 | 17 | 3 | 23 | 3 | 17 | 3 | 22 | 3 | 17 | 3 | 21 | 2 | 25 | 2 | 29 |
| | 4th | 3 | 17 | 3 | 24 | 3 | 17 | 3 | 23 | 3 | 17 | 3 | 21 | 2 | 25 | 2 | 30 |
| | 5th | 3 | 17 | 3 | 25 | 3 | 17 | 3 | 23 | 3 | 17 | 3 | 22 | 2 | 25 | 2 | 31 |
| | 6th | 3 | 17 | 3 | 24 | 3 | 17 | 3 | 23 | 3 | 17 | 3 | 21 | 2 | 25 | 2 | 29 |
| $W = 6$ | 2nd | 3 | 17 | 3 | 31 | 3 | 17 | 3 | 29 | 3 | 17 | 3 | 25 | 2 | 23 | 2 | 31 |
| | 3rd | 3 | 17 | 3 | 29 | 3 | 17 | 3 | 27 | 3 | 17 | 3 | 25 | 2 | 23 | 2 | 30 |
| | 4th | 3 | 17 | 3 | 29 | 3 | 17 | 3 | 28 | 3 | 17 | 3 | 25 | 2 | 23 | 2 | 28 |
| | 5th | 3 | 17 | 3 | 31 | 3 | 17 | 3 | 28 | 3 | 17 | 3 | 25 | 2 | 23 | 2 | 29 |
| | 6th | 3 | 17 | 3 | 28 | 3 | 17 | 3 | 26 | 3 | 17 | 3 | 24 | 2 | 23 | 2 | 30 |

Figure 6 shows the percentage of users migrated from Inter-BBU CoMP to Intra-BBU CoMP at $W = 6$. The figure shows the same performance explained in Figure 4 except for an increased number of migrated users from inter-CoMP to intra-CoMP in each case. This can be explained as follows; increasing the capacities of the links allow a change in serving BBUs for more RRHs and hence, increases the number of migrated users.

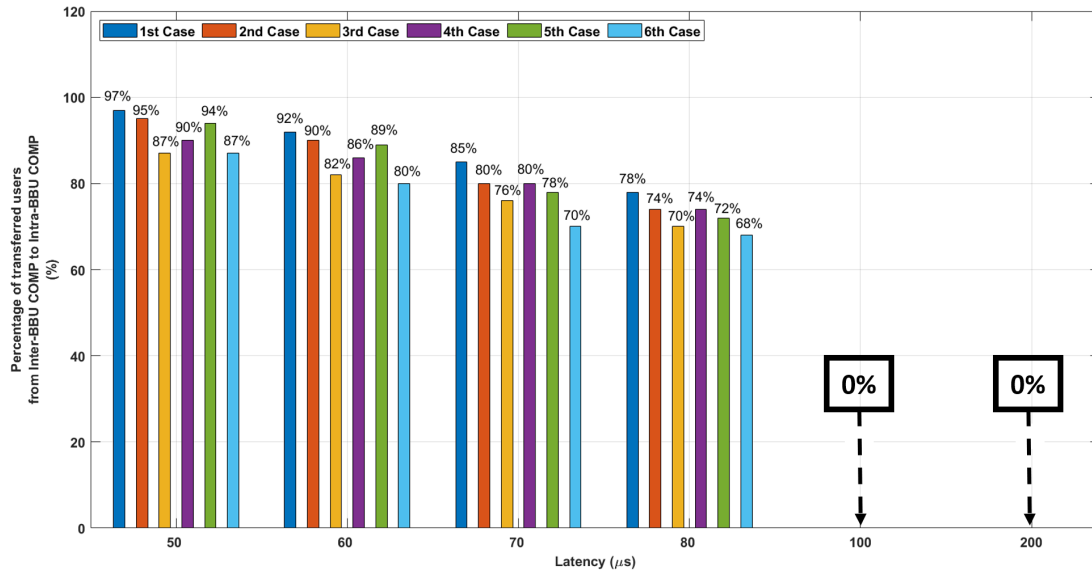


Figure 6. Percentage of transferred users from Inter-BBU COMP to Intra-BBU COMP (for each case, $W = 6$).

Figure 7 shows the number of BBU pools and the number of physical links versus different maximum allowable latency values (D_{max}) at $W = 6$. At 25 μ sec and 35 μ sec, there is no change in the number of BBUs and the number of physical links after the reconfigurable placement of the front-haul links because the maximum delay is not sufficient for re-configuring the RRH to be served by BBU.

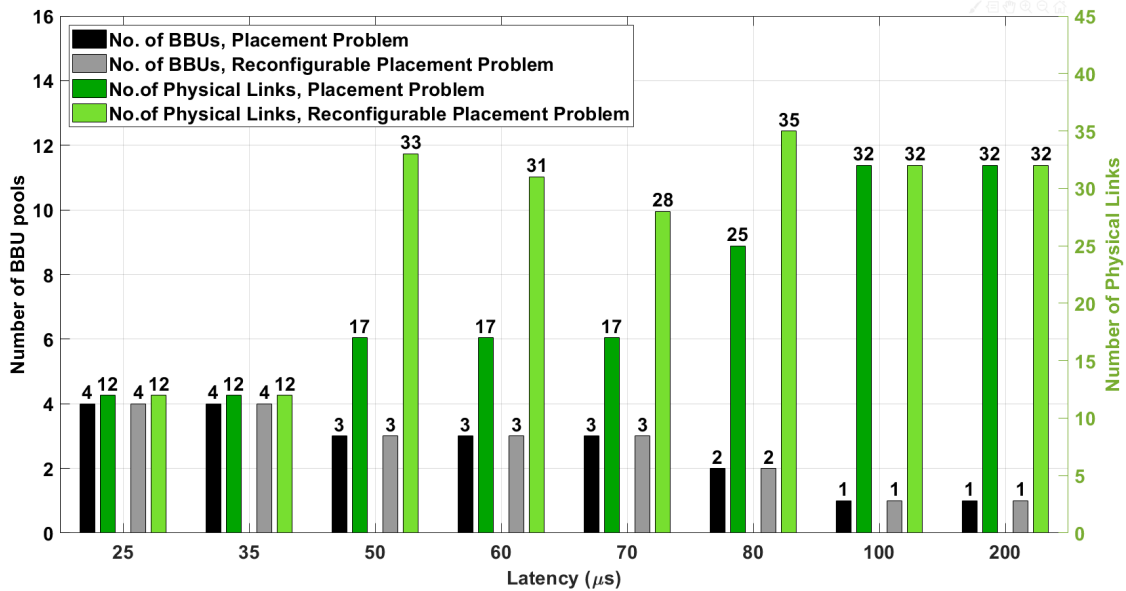


Figure 7. Number of BBU pools and physical links ($W = 6$, 1st case).

At delays equal 50 μ sec, 60 μ sec, and 70 μ sec, the number of BBUs do not change after reconfiguration, while the number of physical links increased by 94%, 82%, and 65% of the optimal solution, respectively. This can be explained by the fact that the maximum allowable delay increases the probability that the adjacent sites are served by the same BBU increase, leading to a higher number of intra-CoMP. Therefore, the number of migrated users decreases, and the number of sites that need to change their served BBU decreases. At delays equaling 80 μ sec, the number of BBUs decreased to two BBUs instead of three in the previous delays. This led to an increase in the number of intra-CoMP as the probability

of sites being served by different BBUs decreases. Therefore, physical links increased by 40%. At delays of 100 μ sec and 200 μ sec, all sites in the area are served by one BBU; as a result, there is no inter-CoMP. Therefore, there is no reconfiguration, and the number of physical links remains constant.

6. Conclusions

In this paper, we proposed a BBU placement problem by taking into consideration the minimization of the number of inter-CoMP users, the number of BBUs, and the number of used wavelengths. First, we formulated an ILP model to place the BBUs and routed the connections, where the objective function is to minimize the number of BBUs and the number of used wavelengths. We took into consideration the link's capacity and trip delay constraints. Second, based on the output of the ILP model, we proposed a heuristic algorithm to relocate the RRHs with respect to the BBUs. The heuristic algorithm aims to reduce the number of inter-CoMP users. We used six different cases in the heuristic algorithm based on the minimum delay path, the minimum number of used fiber links, and the maximum multiplexing gain. The results showed that the maximum gain leads to the highest percentage of migrated users from inter-CoMP to intra-CoMP (97%). On the contrary, this resulted in an increased number of used wavelengths. The used wavelength increased by 94% when compared to the output ILP model. As a result, the overall X2 was minimized. Using Deep Reinforcement Learning (DRL) in the BBU placement problem while decreasing the number of inter-CoMP users can be considered as a future path in research.

Author Contributions: Conceptualization, M.S., S.M.G. and H.E.-B.; Investigation, A.M.A.; Methodology, A.M.A., M.S., S.M.G. and H.E.-B.; Software, A.M.A.; Supervision, M.S., S.M.G. and H.E.-B.; Writing—review & editing, A.M.A., M.S., S.M.G. and H.E.-B. All authors have read and agreed to the published version of the manuscript.

Funding: This research received no external funding.

Conflicts of Interest: The authors declare no conflict of interest.

References

1. Ejaz, W.; Sharma, S.K.; Saadat, S.; Naeem, M.; Anpalagan, A.; Chughtai, N.A. A comprehensive survey on resource allocation for CRAN in 5G and beyond networks. *J. Netw. Comput. Appl.* **2020**, *160*, 102638.
2. Park, J.H.; Rathore, S.; Singh, S.K.; Salim, M.M.; Azzaoui, A.; Kim, T.W.; Pan, Y.; Park, J.H. A comprehensive survey on core technologies and services for 5G security: Taxonomies, issues, and solutions. *Hum.-Centric Comput. Inf. Sci.* **2021**, *11*, 22.
3. Li, H.; Dong, M.; Ota, K.; Guo, M. Pricing and repurchasing for big data processing in multi-clouds. *IEEE Trans. Emerg. Top. Comput.* **2016**, *4*, 266–277.
4. Wang, J.; Jin, C.; Tang, Q.; Xiong, N.; Srivastava, G. Intelligent ubiquitous network accessibility for wireless-powered MEC in UAV-assisted B5G. *IEEE Trans. Netw. Sci. Eng.* **2020**, *8*, 2801–2813.
5. Sangaiah, A.K.; Javadpour, A.; Pinto, P.; Ja'fari, F.; Zhang, W. Improving Quality of Service in 5G Resilient Communication with THE Cellular Structure of Smartphones. *ACM Trans. Sens. Netw. (TOSN)* **2022**, *18*, 1–22. [[CrossRef](#)]
6. Checko, A.; Christiansen, H.L.; Yan, Y.; Scolari, L.; Kardaras, G.; Berger, M.S.; Dittmann, L. Cloud RAN for mobile networks—A technology overview. *IEEE Commun. Surv. Tutor.* **2014**, *17*, 405–426.
7. Habibi, M.A.; Nasimi, M.; Han, B.; Schotten, H.D. A comprehensive survey of RAN architectures toward 5G mobile communication system. *IEEE Access* **2019**, *7*, 70371–70421.
8. Shehata, M.; Elbanna, A.; Musumeci, F.; Tornatore, M. C-RAN baseband pooling: Cost model and multiplexing gain analysis. In Proceedings of the 19th International Conference on Transparent Optical Networks (ICTON), Girona, Spain, 2–6 July 2017; pp. 1–4.
9. Ramírez, S.; Martínez, D.; Zambrano, V.M. Study of the Fronthaul WDM Applied to the Cloud RAN of 5G-CRAN. In Proceedings of the International Conference on Systems and Information Sciences (ICCIS), Manta, Ecuador, 27–29 July 2020; pp. 281–294.
10. Jaffer, S.S.; Hussain, A.; Qureshi, M.A.; Khawaja, W.S. Towards the shifting of 5G front haul traffic on passive optical network. *Wirel. Pers. Commun.* **2020**, *112*, 1549–1568.
11. Wang, X.; Cavdar, C.; Wang, L.; Tornatore, M.; Zhao, Y.; Chung, H.S.; Lee, H.H.; Park, S.; Mukherjee, B. Joint allocation of radio and optical resources in virtualized cloud RAN with CoMP. In Proceedings of the Global Communications Conference (GLOBECOM), Washington, DC, USA, 4–8 December 2016; pp. 1–6.

12. Bellanzon, C. Enhancing Throughput in Centralized Radio Access Network by Intelligent Controller Placement. Master's Thesis, Politecnico Di Milano, Milan, Italy, 2016.
13. Hossain, M.F.; Mahin, A.U.; Debnath, T.; Mosharraf, F.B.; Islam, K.Z. Recent research in cloud radio access network (C-RAN) for 5G cellular systems—A survey. *J. Netw. Comput. Appl.* **2019**, *139*, 31–48.
14. Liu, Q.; Han, T.; Ansari, N.; Wu, G. On designing energy-efficient heterogeneous cloud radio access networks. *IEEE Trans. Green Commun. Netw.* **2018**, *2*, 721–734.
15. Younis, A.; Tran, T.X.; Pompili, D. Bandwidth and energy-aware resource allocation for cloud radio access networks. *IEEE Trans. Wirel. Commun.* **2018**, *17*, 6487–6500.
16. Peng, M.; Wang, C.; Lau, V.; Poor, H.V. Fronthaul-constrained cloud radio access networks: Insights and challenges. *IEEE Wirel. Commun.* **2015**, *22*, 152–160.
17. Musumeci, F.; Bellanzon, C.; Carapellese, N.; Tornatore, M.; Pattavina, A.; Gosselin, S. Optimal BBU placement for 5G C-RAN deployment over WDM aggregation networks. *J. Light. Technol.* **2015**, *34*, 1963–1970.
18. Klinkowski, M. Planning of 5G C-RAN with optical fronthaul: A scalability analysis of an ILP model. In Proceedings of the 20th International Conference on Transparent Optical Networks (ICTON), Bucharest, Romania, 1–5 July 2018; pp. 1–4.
19. Fayad, A.; Jha, M.; Cinkler, T.; Rak, J. Planning a Cost-Effective Delay-Constrained Passive Optical Network for 5G Fronthaul. In Proceedings of the International Conference on Optical Network Design and Modeling (ONDM), Warsaw, Poland, 16–19 May 2022; pp. 1–6.
20. Tinini, R.I.; Reis, L.C.; Batista, D.M.; Figueiredo, G.B.; Tornatore, M.; Mukherjee, B. Optimal placement of virtualized BBU processing in hybrid cloud-fog RAN over TWDM-PON. In Proceedings of the IEEE Conference and Exhibition on Global Telecommunications (GLOBECOM), Singapore, 4–8 December 2017; pp. 1–6.
21. Ahsan, M.; Ahmed, A.; Al-Dweik, A.; Ahmad, A. Functional Split-Aware Optimal BBU Placement for 5G Cloud-RAN Over WDM Access/Aggregation Network. *IEEE Syst. J.* **2022**, *16*, 1–12. [[CrossRef](#)]
22. Yao, J.; Ansari, N. Joint content placement and storage allocation in C-RANs for IoT sensing service. *IEEE Internet Things J.* **2018**, *6*, 1060–1067.
23. Shehata, M.; Musumeci, F.; Tornatore, M. Resilient BBU placement in 5G C-RAN over optical aggregation networks. *Photonic Netw. Commun.* **2019**, *37*, 388–398.
24. Khorsandi, B.M.; Raffaelli, C.; Fiorani, M.; Wosinska, L.; Monti, P. Survivable BBU hotel placement in a C-RAN with an optical WDM transport. In Proceedings of the 13th International Conference Design of Reliable Communication Networks (DRCN), Munich, Germany, 8–10 March 2017; pp. 1–6.
25. Javadpour, A.; Wang, G. cTMvSDN: improving resource management using combination of Markov-process and TDMA in software-defined networking. *J. Supercomput.* **2022**, *78*, 3477–3499.
26. Yang, S.; He, N.; Li, F.; Trajanovski, S.; Chen, X.; Wang, Y.; Fu, X. Survivable Task Allocation in Cloud Radio Access Networks With Mobile-Edge Computing. *IEEE Internet Things J.* **2020**, *8*, 1095–1108.
27. Gao, Z.; Yan, S.; Zhang, J.; Han, B.; Wang, Y.; Xiao, Y.; Simeonidou, D.; Ji, Y. Deep Reinforcement Learning-based Policy for Baseband Function Placement and Routing of RAN in 5G and Beyond. *J. Light. Technol.* **2021**, *40*, 470–480.
28. Mo, W.; Gutterman, C.L.; Li, Y.; Zussman, G.; Kilper, D.C. Deep neural network based dynamic resource reallocation of BBU pools in 5G C-RAN ROADM networks. In Proceedings of the Optical Fiber Communication Conference, San Diego, CA, USA, 11–15 March 2018; pp. 1–4.
29. Qamar, F.; Dimiyati, K.B.; Hindia, M.N.; Noordin, K.A.B.; Al-Samman, A.M. A comprehensive review on coordinated multi-point operation for LTE-A. *Comput. Netw.* **2017**, *123*, 19–37.
30. HAMMODAT, A.N.; AYOUB, S.A. Studying the effect of increasing capacity using comp technology in lte-a networks. *J. Eng. Sci. Technol.* **2021**, *16*, 556–570.
31. Karmakar, R.; Chattopadhyay, S.; Chakraborty, S. A learning-based dynamic clustering for coordinated multi-point (CoMP) operation with carrier aggregation in LTE-advanced. In Proceedings of the 10th International Conference on Communication Systems and Networks (COMSNETS), Bengaluru, India, 3–7 January 2018; pp. 283–290.
32. Bhuvaneshwari, P.; Nithyanandan, L. Improving energy efficiency in backhaul of LTE-A network with base station cooperation. *Procedia Comput. Sci.* **2018**, *143*, 843–851.
33. Musumeci, F.; Bellanzon, C.; Carapellese, N.; Tornatore, M.; Pattavina, A.; Gosselin, S. On the placement of BBU hotels in an optical access/aggregation network for 5G transport. In Proceedings of the Asia Communications and Photonics Conference, Hong Kong, China, 19–23 November 2015; pp. 1–2.
34. Touati, H.; Castel-Taleb, H.; Jouaber, B.; Akbarzadeh, S. Model-Based optimization for JT CoMP in C-RAN. In Proceedings of the IEEE Conference on Computer Communications Workshops (INFOCOM WKSHOPS), Paris, France, 30 April 2019; pp. 403–409.
35. Chen, J.; Ge, X.; Zhong, Y.; Li, Y. A Novel JT-CoMP Scheme in 5G Fractal Small Cell Networks. In Proceedings of the IEEE Wireless Communications and Networking Conference (WCNC), Marrakesh, Morocco, 15–18 April 2019; pp. 1–7.
36. Elhattab, M.; Arfaoui, M.A.; Assi, C. A joint CoMP C-NOMA for enhanced cellular system performance. *IEEE Commun. Lett.* **2020**, *24*, 1919–1923.
37. Awad, M.K.; Baidas, M.W.; Ahmad, A. Optimal Downlink Resource Allocation for Joint Transmission CoMP-Enabled NOMA Networks: A Benchmark Implementation. In Proceedings of the 36th National Radio Science Conference (NRSC), Port Said, Egypt, 16–18 April 2019; pp. 249–258.

38. Yu, Y.J.; Hsieh, T.Y.; Pang, A.C. Millimeter-wave backhaul traffic minimization for CoMP over 5G cellular networks. *IEEE Trans. Veh. Technol.* **2019**, *68*, 4003–4015.
39. Chen, S.; Zhao, T.; Chen, H.H.; Meng, W. Downlink coordinated multi-point transmission in ultra-dense networks with mobile edge computing. *IEEE Netw.* **2018**, *33*, 152–159.
40. Aktar, M.R.; Hossain, M.F.; Al-Hasan, M. Dynamic clustering approach for interference cancellation in downlink C-RAN. In Proceedings of the International Conference on Computer, Communication, Chemical, Material and Electronic Engineering (IC4ME2), Rajshahi, Bangladesh, 8–9 February 2018; pp. 1–4.
41. Chen, Q.; Yang, K.; Jiang, H.; Qiu, M. Joint beamforming coordination and user selection for CoMP enabled NR-U networks. *IEEE Internet Things J.* **2021**, *9*, 14530–14541.
42. Mismar, F.B.; Evans, B.L. Deep learning in downlink coordinated multipoint in new radio heterogeneous networks. *IEEE Wirel. Commun. Lett.* **2019**, *8*, 1040–1043.
43. Shami, T.M.; Grace, D.; Burr, A.; Zakaria, M.D. Joint User-Centric Clustering and Multi-cell Radio Resource Management in Coordinated Multipoint Joint Transmission. *Wirel. Pers. Commun.* **2022**, *124*, 2983–3011.
44. Musumeci, F.; De Silva, E.; Tornatore, M. Enhancing RAN throughput by optimized CoMP controller placement in optical metro networks. *IEEE J. Sel. Areas Commun.* **2018**, *36*, 2561–2569.
45. Zhang, J.; Ji, Y.; Jia, S.; Li, H.; Yu, X.; Wang, X. Reconfigurable optical mobile fronthaul networks for coordinated multipoint transmission and reception in 5G. *IEEE/OSA J. Opt. Commun. Netw.* **2017**, *9*, 489–497.
46. Shehata, M.; Elbanna, A.; Musumeci, F.; Tornatore, M. Multiplexing gain and processing savings of 5G radio-access-network functional splits. *IEEE Trans. Green Commun. Netw.* **2018**, *2*, 982–991.
47. Khorsandi, B.M.; Tonini, F.; Raffaelli, C. Centralized vs. distributed algorithms for resilient 5G access networks. *Photonic Netw. Commun.* **2019**, *37*, 376–387. [[CrossRef](#)]